# Accepted Manuscript


Molecular and supramolecular helicity induction in trityl group-containing compounds: The case of chiral 3,3,3-triphenylpropionic acid derivatives

Paweł Skowronek, Agnieszka Czapik, Zuzanna Rajska, Marcin Kwit

PII: S0040-4020(19)30712-4

DOI: https://doi.org/10.1016/j.tet.2019.06.040

Reference: TET 30432

To appear in: *Tetrahedron*

Received Date: 18 April 2019

Revised Date: 21 June 2019

Accepted Date: 24 June 2019

Please cite this article as: Skowronek Paweł, Czapik A, Rajska Z, Kwit M, Molecular and supramolecular helicity induction in trityl group-containing compounds: The case of chiral 3,3,3-triphenylpropionic acid derivatives, *Tetrahedron* (2019), doi: https://doi.org/10.1016/j.tet.2019.06.040.

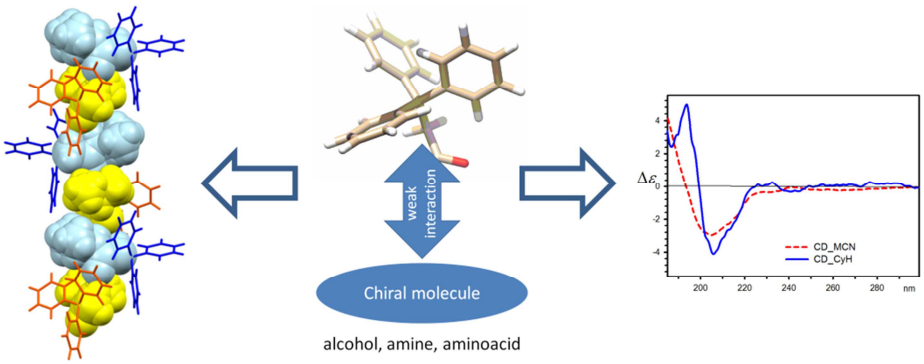

# Molecular and supramolecular helicity induction in trityl group-containing compounds: the case of chiral 3,3,3-triphenylpropionic acid derivatives

Paweł Skowronek,*[a] Agnieszka Czapik,[a,b] Zuzanna Rajska[a] and Marcin Kwit*[a,b]

a) Department of Chemistry Adam Mickiewicz University, Uniwersytetu Poznańskiego 8, 61 614 Poznań, Poland
b) Centre for Advanced Technologies Adam Mickiewicz University, Uniwersytetu Poznańskiego 10, 61 614 Poznań, Poland

e-mail: skowron@amu.edu.pl or marcin.kwit@amu.edu.pl

**Keywords**

amino acids, chirality, induced optical activity, propeller, structure, trityl group

**Abstract**

The process of dynamic chirality transmission from permanent chirality element to stereodynamic triphenylmethyl group placed in the distance of 4 bonds, has been studied for series of optically active 3,3,3-triphenylpropionic acid derivatives. Structural analysis, carried out with the use of complementary methods and supported by theoretical calculations, enabled us to determine the mechanism of chirality transmission. The observed chirality transfer phenomenon, demonstrated unequivocally as raising of non-zero Cotton effects in the region of UV absorption of trityl group, is a cascade process driven by weak intramolecular interactions. Despite the much larger inductor-effector distance, the sensitivity in chirogenesis is comparable to other stereodynamic probes reported so far. In the crystalline phase, the combination of trityl group with amino acid moiety results in the formation of helical superstructures, where individual molecules are held together by hydrogen bonding cascades. The proper combination of functionalities in the molecule skeleton allows, to some extent, the control over the association process and authorizes determination of the trityl group as the supramolecular synthon.

## 1. Introduction

Induction, control, detection and determination of chirality, together with interactions between chiral objects, are the basis for the stereoselective synthesis, some analytical techniques and chiroptical spectroscopy.[1-4] Chiral molecules resembling macroscopic mechanical devices, such as bevel gears, ratchets and propellers, are still of growing interest to many research groups.[5-7] The

intense studies on the propeller-like group of compounds have been initiated by Mislow and Iwamura. Now, the results of these pioneering works have been recognized as important steps in development of more sophisticated molecular machines fueled by external energy source.[8-11]

One of the most important representative of molecular propellers – the triphenylmethyl group (trityl, Tr) is widely used in synthesis, mostly for protection of polar functionalities such as OH, NH, SH.[12] Recently, Franzén and others have proven utility of stable trityl cations as catalysts in organic synthesis.[13-17] Combination of amino acids and trityl group led to *N*-tritylamino acid derivatives acting as cytostatics,[18-20] exchange-coupled biradicals,[21] and as stationary phases in ligand-exchange chromatography.[22]

Structurally, the mother triphenylmethane molecule consists of three phenyl rings (blades) connected to the central $sp^3$-hybridized carbon atom (hub) residing on the propeller axis. The triphenylmethane and its TrX congeners (where X is a spherically-symmetrical substituent), might adopt two extreme, low-energy enantiomerical, $C_3$-symmetrical conformations. Qualitatively, the rings twist is conveniently determined by either *P* or *M* helicity. The other diastereoisomeric conformations are characterized by different blade angle and by higher relative energy.[23] Triphenylmethane and its simple derivatives form dynamic racemates with low enantiomerization barrier estimated as ca. 5 kcal $mol^{-1}$. The twist of the phenyl rings is preserved also in the triphenylmethyl cation and the energy barrier between the enantiomeric structures of the *P* and *M* helicity has been estimated as 9.1 kcal $mol^{-1}$.[23-26]

The twisted phenyl rings in the trityl moiety form non-planar (chiral) system consisting of three independent but interacting chromophores, which in principle, should led to the rise of non-zero Cotton effects (CEs) in the electronic circular dichroism (ECD) spectra and in the region of ultraviolet (UV) absorption of the chromophore. In the case of triphenylmethane, the mutual contributions of enatiomeric *P*- and *M*-helical conformers cancel CEs to zero, hence, no ECD spectrum is observed. However, the connection of trityl group to the non-spherically symmetrical and chiral substituent disturbs the local symmetry of the trityl chromophore and has led to the generation of non-zero CEs of the characteristic pattern. Such induction of chirality (helicity) has been previously observed for *O*-trityl alcohols, *N*-trityl amines, sulfides and selenides, triphenylacetic acid derivatives and related compounds.[27-32] Thus, the observed chirality transfer from permanent chirality element to the dynamically chiral chromophore allows to classify trityl as stereodynamic chirality probe.[33]

The so far proposed models of optical activity connect the signs of observed CEs (and helicity of the triphenylmethane chromophore) with the steric power of substituents flanking stereogenic center, which is not always directly related to the absolute configuration of the chirality element.[27-32] In

particular, the induction of optical activity in *O*-trityl alcohol and *N*-trityl amines results from the direct gearing between trityl and inductor fragment ("a bevel gear" mechanism). Interestingly, a similar chirality transfer from chiral alcohols to the *O*-triphenylsilyl group has been recently reported.[34] More subtle interactions involving C–H/C=O(amide) dipoles together with C-H$\cdots\pi$ and O$\cdots$H-C electrostatic attractive interactions are responsible for the chirality transfer in mono and bis(triphenylacetamides).[30,31]

Recently, we and others have shown that trityl moiety might play an important role in the crystal engineering as a supramolecular protecting group that precludes formation of hydrogen bonded aggregates in the crystalline phase. Even in the enantiomerically pure crystals, the symmetry independent part of the unit cell contain the molecules characterized by opposite helicity of the trityl fragments, which exhibit tendency to form aggregates made from pairs of pseudocentrosymmetric dimers.[35]

On the other hand, the poor shape complementarity of some trityl derivatives led to the low-density crystals, in which empty voids are formed, that may or may not be occupied by the guest molecules. Akazome has proven possibility of chiral recognition by crystals of tritylated amino acid derivatives.[36,37]

Feeling that the problem of the interplay between permanent chirality element and stereodynamic trityl reporters is still at the initial stage of research, we decided to expand the studies on the derivatives, where the process of chirality transmission precedes among larger inductor-reporter distance. We chose the 3,3,3-triphenylpropionic acid as a reporter system, that will be modified by transformation into chiral esters and amides including amino acid derivatives. In these cases, the distance between the inductor and the reporter (i.e. 4 bonds) is larger than in previously reported *O*-tritylethers and *N*-tritylamines (2 bonds distance) and triphenylacetic acid derivatives (3 bond distance). We are hoping that the detailed mechanism of the generation of optical activity in selected derivatives will be established by ECD spectroscopy supported by theoretical calculations at the DFT level. The effectiveness of the chirality transfer from permanent chirality element to the stereodynamic trityl probe is proportional to the magnitude of induced CE's. However, the convenient way to compare sensitivity in chirogenesis between different molecular or supramolecular systems, is to compare their dissymmetry factors *g*, that are defined as $\Delta\varepsilon/\varepsilon$ ratio at a given wavelength.[3]

Elongation of the carbon chain in 3,3,3-triphenylpropionic acid can significantly affect the way of molecular packing of its chiral derivatives in the crystal. Especially, due to liberation of secondary amide supramolecular synthon from a protective umbrella of trityl fragment, the molecular

association can be governed by hydrogen bonding cascades. The response of the trityl fragment to the association and, therefore, the possibility to form dense or low-density crystals capable of inclusion, is also worth mentioning. The latter problem is crucial to the rational planning of new chiral materials of defined (i.e. sorption) properties.

## 2. Results and discussion

### *2.1. Synthesis.*

The starting 3,3,3-triphenylpropionic acid has been obtained according to the procedure of Hellerman,[38] by first melting triphenylmethanol with malonic acid and subsequent treatment of melted alloy with sodium hydroxide to separate unreacted triphenylmethanol and then with an excess of hydrochloric acid (**Scheme 1a**). The methyl esters of selected amino acids were prepared according to the known procedures.[39] The representative series of chiral 3,3,3-triphenylpropionic acid esters **1**, amides **2** and *N*-(3,3,3-triphenylpropionyl)amino acid derivatives **3**-**4**, have been conveniently obtained from alcohol, amine, amino acid ester or from free amino acid and 3,3,3-triphenylpropionyl chloride. Yields of the reactions were varied from good to moderate and the products were easily purified either by crystallization or by flash column chromatography. Exemplary synthetic procedures were shown in the Experimental section; the remaining results including full spectroscopic characteristics of the new compounds were deposited as supplementary material.

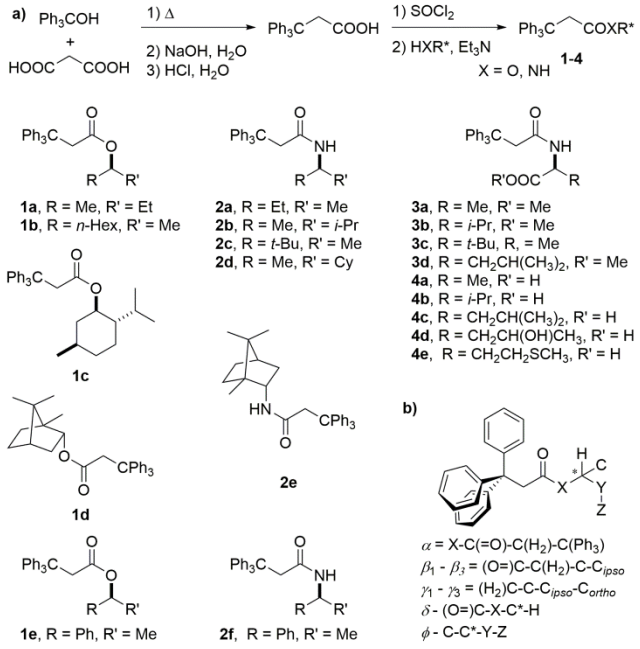


**Scheme 1.** a) General procedure for synthesis of the optically active derivatives of 3,3,3-triphenylpropionic acid **1**-**4**. b) Definition of dihedral angles that characterize the molecular conformation.

### *2.2. ECD spectra and mechanism of chirality transmission in 3,3,3-triphenylpropionic acid derivatives 1-4.*

Having obtained the optically active derivatives **1**-**4**, we were able to study the possibility of chirality transmission from stereogenic center to the stereodynamic trityl chromophore. For convenient sensing of the induced optical activity in the trityl chromophore, we used the ECD spectroscopy as the method of choice. Additionally, in our studies, we have taken an opportunity of hydrophobicity of these compounds, since the solubility in the non-polar hydrocarbons will facilitate further theoretical analysis. This approach allows us to direct comparison of experimental ECD results with theoretical ones obtained for molecules calculated *in vacuo*.[40] In particular, we will focus on derivatives characterized by the presence of aliphatic inductor moieties, since for these derivatives the observed CEs should originate from induced chirality in the chromophore. Both, the –COOR ester group and –CONHR amide group alone are recognized as weak UV active chromphores. The π-π* transition in ester and amide chromophore is separated from the strong $^{1}$B band (195-210 nm) in phenyl rings by distance as well as by energy difference, which makes transitions coupling weak and does not led to generation of intense Cotton effects. It implies that the influence of ester and amide chromophores on the prospective UV and ECD effects might be treated as negligible.[3,41]

In general, for all compounds under study, we observed generation of optical activity in the stereodynamic probe, which is revealed by raising non-zero CEs in the spectral region of trityl absorption (see **Table 1** and **Figure 1**). Taking into account the significantly larger distance between inductor and effector (reporter), the measured induced CEs, although lower than for previously reported derivatives, might by recognized as those of unexpectedly high magnitudes. The natural correlation between the pattern of the spectrum and absolute stereochemistry of the given compound is straightforward in the majority of the cases. For instance, the sign of Cotton effects appearing at about 204 nm seems to be ruled by absolute configuration at stereogenic center. For ester derivatives **1a** and **1b**, aliphatic amides **2a**-**2d** and amino acid derivatives **3a**-**3d** and **4b**-**4f**, a negative sign of this particular CE and positive of the higher-energy CE (if visible) corresponds to *S* configuration and *vice versa*. In the remaining cases, the correlations are not obvious due to the presence of additional chirality elements or chromophoric groups such as phenyl ring.

The amplitude of the observed CEs can be related to the steric bulk of substituents at stereogenic center, as it is particularly seen for amides **2a**-**2c**. The increase of the number of methyl group attached to the carbon atom directly translates to the magnitude of the Cotton effect, i.e. for amide **2c** the observed CE at around 204 nm is over three times as big as that measured for **2a**. The

experimental results suggest that for aliphatic amides the steric power of substituents in the dynamic induction of chirality rises as follows: Me < Et ≈ Cy < *i*-Pr < bornyl < *tert*-Bu.

The presence of an additional aromatic chromophore in inductor skeleton makes the ECD spectrum more difficult to the unequivocal interpretation. In the case of **2f**, the presence of phenyl ring increases the intensity of the UV absorption maximum, whereas in the ECD spectrum, it manifests itself as a negative Cotton effect around 215 nm, not well-separated from the main Cotton effect appearing at around 200 nm. It has been known that the model *N*-pivaloyl amide of (*S*)-1-phenylethylamine is characterized by one negative CE appearing at 197 nm, in the same region where negative CE is observed for **2f**.[30] This suggests a dominant role of over induced CE to the net ECD spectrum of **2f** in the lower-energy region, whereas the short-wavelength CE is rather dominated by induced CE within trityl chromophore.

**Table 1**. Absolute configurations (*AC*) at stereogenic centers, ECD ($\Delta\varepsilon$) and UV ($\varepsilon$) data and dissymmetry factors $g$ ($\Delta\varepsilon/\varepsilon \times 10^{-4}$) for 3,3,3-trifenylpropionic acid derivatives **1**-**4** measured in cyclohexane solution (see also **Table S_1** for remaining data).

| Cmpd. | *AC* | $\Delta\varepsilon$ (nm) | $\varepsilon$ (nm) | $g$ | Cmpd. | *AC* | $\Delta\varepsilon$ (nm) | $\varepsilon$ (nm) | $g$ |
|---|---|---|---|---|---|---|---|---|---|
| **1a** | *R* | +5.0 (203) | 77900 (197) | 0.64 | **2f** | *S* | -7.8 (215); -14.8 (202); +20.8 (188) | 105000 (189) | -1.41 |
| **1b** | *S* | -2.9 (204); +0.2 (196); -1.6 (188) | 78300 (198) | 0.02 | **3a** | *S* | 4.8 (225); -28.9 (204); 18.4 (190) | 92500 (194) | -3.12 |
| **1c** | *R* | +2.4 (227); -6.5 (197) | 75800 (196) | -0.76 | **3b** | *S* | 4.1 (226); -20.9 (203); 12.4 (187) | 82500 (194) | -2.53 |
| **1d** | *S* | +1.0 (228); -0.14 (218); +2.8 (204); -2.3 (196); +4.3 (187) | 71000 (196) | -0.32 | **3c** | *S* | 5.4 (224); -12.2 (203); 1.9 (186) | 84400 (195) | -1.44 |
| **1e** | *S* | -11 $(209)_{sh}$; -16.6 (198) | 124000 (189) | -1.34 | **3d** | *S* | 6.8 (225); -15.9 (205); 11.4 (185)[a] | 82400 (195) | -1.93 |
| **2a** | *S* | -4.1 (205); +4.9 (194) | 80540 (192) | 0.61 | **4a** | *S* | n .a.[b] | n .a.[b] | |
| **2b** | *R* | +10.3 (206); -8.7 (192) | 76720 (194) | -1.14 | **4b** | *S* | 3.7 (226); -10.8 (200); 3.7 (187) | 77900 (195) | -1.38 |
| **2c** | *S* | -17.6 (206); +12.5 (192) | 81350 (193) | 1.54 | **4c** | *S* | 2.2 (226); -11.6 (203); 4.2 (187) | 77300 (195) | 1.50 |
| **2d** | *R* | +5.7 (204); -4.2 (193) | 73300 (192) | -0.57 | **4d** | *S* | n. a.[b] | n .a.[b] | |
| **2e** | *S* | -5.0 (223); +10.1 (193) | 76900 (193) | 1.31 | **4e** | *S* | 2.8 (226); -13.7 (204); 8.9 (187) | 79100 (194) | 1.73 |

[a] The end of measurement range. [b] Data not available due to the poor solubility in cyclohexane.

The same trend as it is seen for amides **2a**-**2c** is observed for derivatives **4b**-**4e**. The increase of molecular complexity of the aliphatic substituent attached to the stereogenic manifests itself in increasing the amplitude of the corresponding Cotton effects.

Surprisingly, a reverse relationship has been found for amino acid derivatives **3a**-**3d**. The characteristic feature for these compounds is step-wise decreasing of the magnitude of the CE appearing at around 205 nm associated with gradual increase of the alkyl backbone size. This might suggest that the increase of the aliphatic substituent size balances the steric bulk of carbomethoxy COOMe group. In the case of **3a**-**3d** and **4b**-**4e**, the first positive long-wavelength CE at around 230 nm is clearly distinguishable. Note, for some compounds, due to the measurement condition restriction (instrument sensitivity and solvent absorption), a maximum of the short-wavelength Cotton effect was not reached and positive values presented in **Table 1** show rather a tendency of the CD curve and not the maximum achieved.

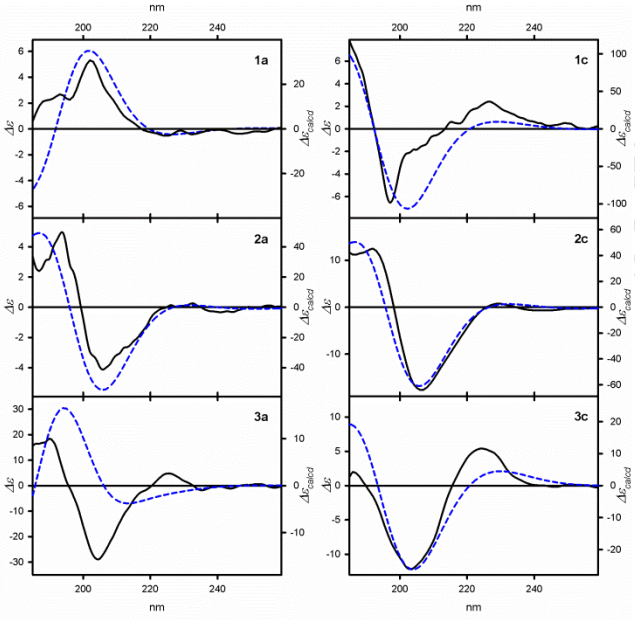


**Figure 1.** Exemplary ECD spectra of chiral triphenylpropionic acid derivatives **1a**, **1c**, **2a**, **2c**, **3a** and **3c**, experimental, measured in cyclohexane (solid black lines) and calculated at the TD-CAM-B3LYP/6-311++G(d,p) level and *ΔΔG*-based Boltzmann averaged (dashed blue lines). Calculated ECD spectra were wavelength corrected to match experimental UV maxima.

Theoretical studies, carried out for selected 3,3,3-trifenylpropionic acid derivatives **1a**, **1c**, **2a**, **2c**, **3a** and **3c**, have shed light on the structure and mechanism of chirality transmission (for calculation details see ESI).[42] The structure of each individual conformer of **1a**, **1c**, **2a**, **2c**, **3a** and **3c** can be conveniently described by a set of angles $\alpha - \varphi$ (defined in **Scheme 1b)** and juxtaposed in **Table S_3** in Supplementary Info. The angle $\alpha$ (X-C(=O)-C($H_2$)-C) characterizes the conformation of the reporter carbon chain, which is directly related to the inductor-effector distance. The angles $\beta_1 - \beta_3$ ((O=C)-

$C(H_2)$-C-$C_{ipso}$) and $\gamma_1 - \gamma_3$ ($C(H_2)$-C-$C_{ipso}$-$C_{ortho}$) describe the conformation of phenyl groups. The first set describes the orientation the phenyl rings with respect to the alkyl chain whereas the second characterizes the helicity of the Tr fragment. The angles $\gamma_1 - \gamma_3$ define helicity of the blades: *M* (-90° < $\gamma$ < 0°), *P* (0° < $\gamma$ < 90°) or *0* (for $\gamma$ angles deviating from zero by less than 5°). The angles $\delta$ and $\varphi$, respectively, describe mutual relationship between inductor and effector skeletons and conformation of an inductor.

Despite the expected larger conformational freedom of 3,3,3-trifenylpropionic acid derivatives, the number of low-energy conformers (see **Table S_2**) is comparable to that established previously for more rigid chiral triphenylacetic acid amides.[30] The structures of *ΔΔG*-based lowest energy conformers of **1a**, **1c**, **2a**, **2c**, **3a** and **3c** have been shown in **Figure 2** (the remaining structures of low-energy conformers are deposited in ESI).

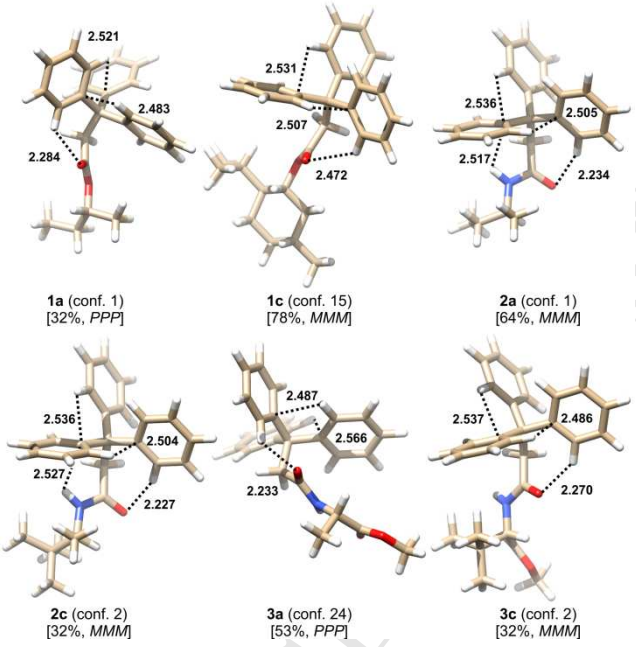


**1a** (conf. 1) [32%, *PPP*] **1c** (conf. 15) [78%, *MMM*] **2a** (conf. 1) [64%, *MMM*]

**2c** (conf. 2) [32%, *MMM*] **3a** (conf. 24) [53%, *PPP*] **3c** (conf. 2) [32%, *MMM*]

**Figure 2.** Structures of *ΔΔG*-based the lowest energy conformers of **1a**, **1c**, **2a**, **2c**, **3a** and **3c**, calculated at the B3LYP/6-311++G(d,p) level. In the square brackets percentage population of given conformer and helicity of the trityl moiety are provided. Dashed lines indicate possible attractive interactions that control conformation of the trityl groups. Distances are in angstroms.

Conformation of the reporter chain, defined by the α angles, varied from ±*anticlinal* (*ac*) to +*synclinal* (*sc*). The latter are especially visible for amide derivatives **2a** and **2c**. To minimize the torsion strains, the phenyl rings are placed consequently ±*antiperiplanar* (*ap*) and ±*sc*, as analysis of *β* angle conformations revealed. Similar conformation of trityl group is observed for triphenylethane and other trityl derivatives substituted by achiral substituent of spherical symmetry. The low-energy conformers of **1a**, **1c**, **2a**, **2c**, **3a** and **3c** are characterized by *MMM* or *PPP* helicity of phenyl rings, where conformation of two of three phenyl rings are ±*sc* and the third one is ±*synperiplanar* (*sp*).

Further flattening of the third *γ* angle (up to *0* helicity) is associated with an increase in energy of the given conformer. With no exceptions, the *δ* angles adopt *sp* conformation. This is due to the attractive C=O···H-C* dipole-dipole interactions, which strongly stabilize the structure and determine orientation of the substituents at the stereogenic center in space. Statistically, the angle *φ* adopts ±*ap* and ±*sc* conformation in the case of ester derivative **1a**, and ±*sc* or ±*ac* conformation in amino acid derivatives **3a** and **3c**.

However, even the most detailed description of the angles does not give the view on the chirality transfer mechanism. The carried out theoretical analysis indicates the subtle electrostatic C=O···H-$C_{ortho}$ interactions as the decisive factor for the efficiency of the chirality transfer. The calculated C=O···H-$C_{ortho}$ distances ranging from 2.150 Å to 2.794 Å, and the shorter ones are characteristic for conformers with lower relative energies. The C=O···H-$C_{ortho}$ interactions control *sp* conformation of one of the phenyl rings from the trityl moiety. Conformation of the remaining phenyl groups is controlled mostly by the $C_{ortho}$-H···$C_{ipso}$ interactions and, to less extend, by sterical interactions with substituents attached to the stereogenic center. In the case of the lowest energy conformers of secondary amides **2a** and **2c**, the attractive N-H···π interactions seem not to be less important than the C=O···H-$C_{ortho}$ interactions for controlling the molecular conformation. In these particular cases, the third propeller blades are forced to adjust their conformation to the remaining two.

Confrontation of the structural data with calculated ECD spectra for each low-energy conformer of **1a**, **1c**, **2a**, **2c**, **3a** and **3c** clearly indicate that *MMM* helicity of the propeller is associated with positive-negative-positive (+/-/+) sequence of CEs, whereas for *PPP* helicity a reversed order -/+/- of CEs is established by theoretical calculations.

The correctness of the theoretical analysis has been confirmed by the direct comparison of experimental and theoretical ECD spectra of the model compounds **1a**, **1c**, **2a**, **2c**, **3a** and **3c** (see **Figure 1**). The agreement between experimental and theoretical results is very good, with the exception of amide **3a**, representing indeed a very complex system. In line with expectations, the *ΔΔG*-based and Boltzmann averaged theoretical ECD spectra of **1a**, **1c**, **2a**, **2c** and **3c** are dominated by the lowest-energy and, therefore, the most abundant conformer. The ECD spectrum calculated for the *ΔΔG*-based lowest energy conformer of **3a**, characterized by *PPP* helicity of the chromophore, remains in disagreement with the experiment. However, the calculated and Boltzmann averaged ECD spectrum of **3a** is influenced by higher energy conformers (mainly by the second lowest-energy conformer no 39) characterized by *MMM* helicity of Tr moiety (see **Figure 3**). As the population of these structures is underestimated, the averaged theoretical ECD spectrum of **3a** remains in fair agreement with the experimental one.

It is worth emphasizing that within the series of model compounds **1a**, **1c**, **2a**, **2c**, **3a** and **3c**, the structure of the chiral inducer and the presence of chromophores different than Tr ones, have small or even negligible contribution to the overall ECD spectrum (see **Figure 3b**).

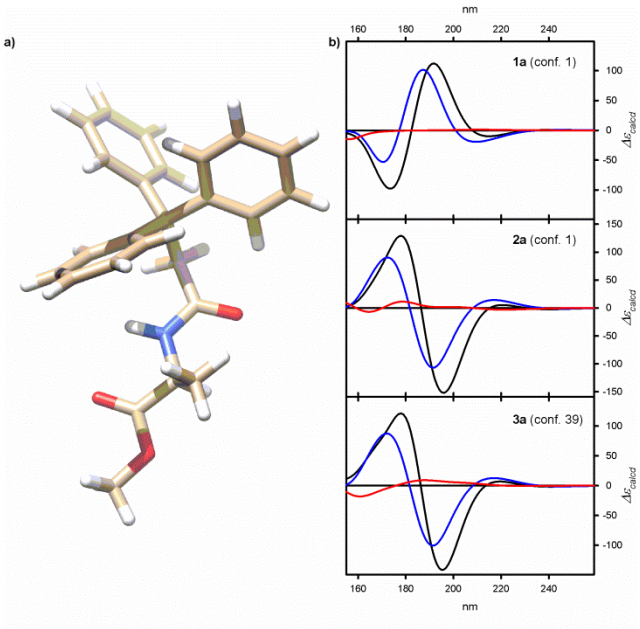


**Figure 3.** a) Structure of low-energy conformer no 39 of amide **3a**, calculated at the B3LYP/6-311++G(d,p) level. b) Exemplary "depuzzled" ECD spectra calculated for *ΔΔG*-based low-energy conformers of **1a**, **2a** and **3a** (solid black lines), their trityl parts only (solid blue lines) and their non-aromatic parts only (solid red lines). Wavelengths were not corrected.

### *2.3. Molecular and supramolecular structures of chiral amides of 3,3,3-triphenylpropionic acid as revealed by X-ray crystallography*

The reported here crystal structures of chiral 3,3,3-triphenylpropionic acid derivatives **2a**-**2c**, **3a**-**3c** and **4a** were analyzed taking into account their molecular and supramolecular structures. Due to the formally larger distance between the inductor and the effector, we are expecting lesser influence of hydrophobic trityl group on the structure of possible associates than it has been found for respective triphenylacetic acid derivatives. In addition to the most common secondary amide supramolecular synthon, the presence of free carboxylic group might lead to formation of various supramolecular assemblies. Therefore, from the compounds under study, the 3,3,3-triphenylpropionic acid derivatives of amino acids are of the special attention. The summary of crystallographic data is given in **Table S_4** and selected X-ray structural data are juxtaposed in the **Table S_5** in ESI. The molecular structure of compounds **2a**-**2c**, **3a**-**3c** and **4a** in crystals are presented in **Figure S_44-S_50**.

The general and characteristic feature of all compounds under study is their large structural diversity in the solid state. The molecules in the crystalline phase adopt extended conformation of the effector fragment (the *α* angles are *ap*). In the crystal structures of compounds **2a**-**2c** and **3a**-**3c**, amide groups

are involved in the N-H···O=C hydrogen bonds cascade to form a structural 1D motif (for hydrogen bonds geometry see **Table S_6**). Due to the large volume of the trityl group it is impossible to create a flat structure and observed molecular ribbon is twisted with trityl groups arranged helically on the shore (**Figure 4a**). The ribbon structure in the crystals is stabilized by additional intermolecular weak C-H···O=C interactions.

In the crystal structure of compounds **2a** and **2b**, the asymmetric units consist of two independent molecules. The differences in molecular conformation are observed mainly for trityl groups, which are close to the mirror images (for compound **2a** see **Figure 4** b, for compound **2b** see **Figure S_45,** ESI). Conformation of molecule is stabilized by intramolecular $C_{ortho}$-H···O=C hydrogen bonds (2.34 Å and 2.79 Å for **2a**, 2.35 Å and 2.81 Å for **2b**) and structure of twisted ribbon is assisted by intermolecular $C_{ortho}$-H···O=C interactions.

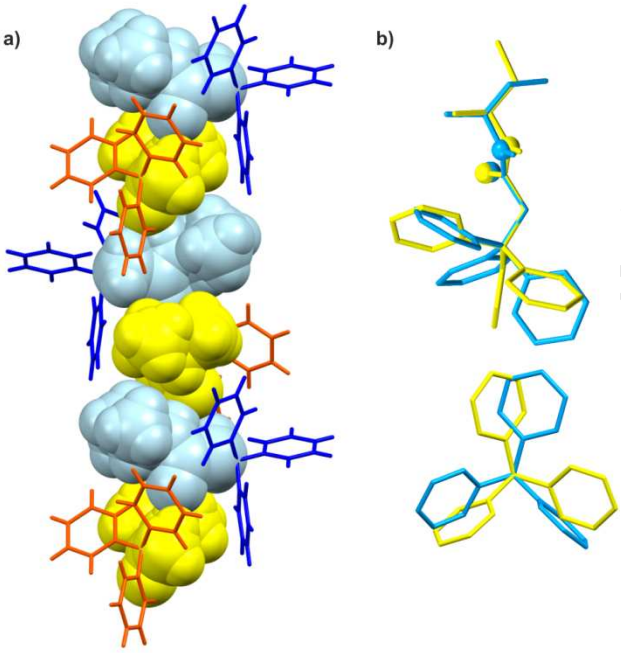


**Figure 4.** a) The twisted-ribbon 1D motif in the crystal structure of **2a**. b) The comparison between the conformation of symmetrically independent molecules A and B. The O and N atoms are shown as balls, C-bound hydrogen atoms have been omitted for clarity. Symmetrically independent molecules are indicated with different colors.

In the crystal of amide **2c** (**Figure 5a**), the asymmetric unit consist of four symmetrically independent molecules A, B, C, D. In the crystalline phase, they are linked *via* N-H···O=C hydrogen bonds to form two independent 1D motifs with a sequence ...ABABA... and ...CDCDC... respectively. The molecules A and B (or C and D), forming one column, are pseudo-symmetric. For the corresponding molecules A and C (or B and D) forming the symmetrically independent columns, the pseudo-symmetry applies only to trityl groups (see **Figure 5b**). In contrast to the previous ones, the trityl groups are not

arranged helically around the column, but they are placed on one side of the column (see **Figure 5a**). The three-dimensional structure is stabilized by C-H··· π interactions between adjacent columns.

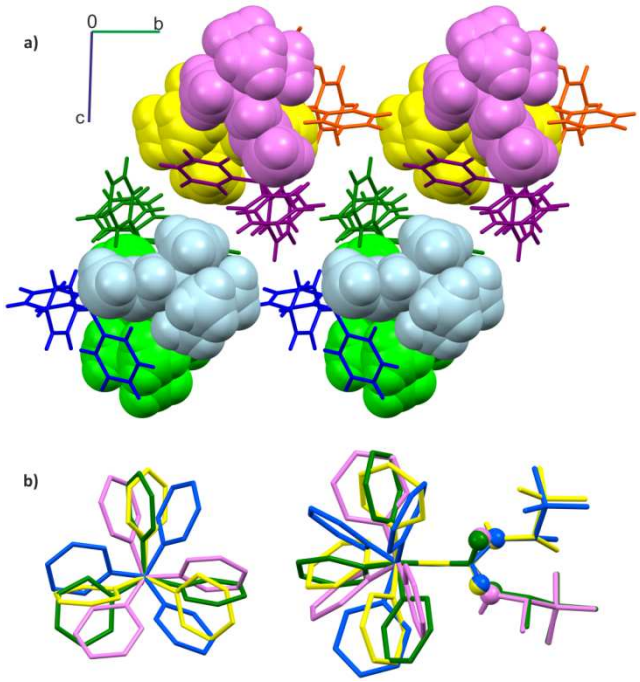


**Figure 5.** a) Molecular packing in the crystal structure of amide **2c**, view along x axis. b) The comparison between the conformations of symmetrically independent molecules A, B, C and D. The O and N atoms are shown as balls, hydrogen bonds are shown as dashed line and C-bound hydrogen atoms have been omitted for clarity. Symmetrically independent molecules are indicated with different colors.

In the crystals of *N*-(3,3,3-triphenylpropionyl)alanine and *N*-(3,3,3-triphenylpropionyl)valine methyl esters (**3a** and **3b**, respectively), two independent molecules were found. The conformation of these independent molecules, do not differ significantly from each other. The twisting angles of phenyl groups ($\gamma_1$ – $\gamma_3$) are of similar value in both cases (-77.3(2), -31.7(2), 20.0(2) and -70.9(2), 11.1(2),-37.6(2) for **3a** and -76.9(2), 18.3(2), -32.7(2) and -67.9 (2), 17.2 (2), -37.5 (2) for **3b**). Such *MPM* arrangement of $\gamma_1$ – $\gamma_3$ angles has not been found for the calculated *in vacuo* low-energy conformers of **2a**.

The conformation of the trityl group is ordered mainly by intermolecular interactions. However, some intramolecular interactions were found as well. In the case of **3b**, the C-H···π intramolecular attractive interactions are postulated. In the crystal state, the molecules of **3b** differ mainly in the position of isopropyl group in the valine backbone. In one of the independent molecules, the methine hydrogen atom of the *i*-Pr group is almost perpendicular to the plane of phenyl ring and it is directed towards the center of the ring (the distance to the center of the phenyl ring is 2.63 Å, the distance to the plane of the phenyl ring is 2.56 Å). For the second molecule, where methine hydrogen is in the opposite direction, a similar interaction with hydrogen atom from the one *i*-Pr methyl group can be proposed. In this particular case, the arrangement is not perfect (the distance to center of the

phenyl ring is 2.59 Å, the distance to the plane of the phenyl ring is 2.56 Å) and C-H bond is not perpendicular to the plane of the aromatic ring. As a result, a significant distortion (by 30°) of *γ* angles from the optimal value (around ±40°) established for simple triphenylmethane has been noticed.

In the case of **3a**, the C-H···π interactions between hydrogen atom from methyl group of alanine backbone (which is equivalent to methine hydrogen atoms in **3b**) and π-electron clouds are weaker.

Similar type of supramolecular architecture has been found in the crystals of **3c**. In this case, in the asymmetric unit 5, independent structures were found. These molecules differ mainly in conformation of the trityl group. While one of the *γ* angles is always negative, the remaining phenyl rings adopted various *M* and *P* conformations.

In the crystal of *N*-(3,3,3-triphenylpropionyl)alanine (**4a**) two independent molecules are observed. The characteristic feature of these molecules is their pseudo-symmetry. Trityl groups in these conformers are almost mirror images (deviation of the *γ* angles is less than 10°) and exhibit either *PPP* or *MMM* helicity. A dominant force in determination of trityl groups conformation are weak intramolecular C-H···O and intermolecular C-H···π interactions.

Crystal structure of **4a** is determined by strong O-H···O hydrogen bonds cascades between neighboring molecules and linking hydrogen atom from carboxylic group with oxygen from the amide group of the second molecule. In contrast to the methyl esters of amino acids, the hydrogen atom from NH amide group in **4a** is not involved in hydrogen bonding. This is due to the shielding effect of the trityl group, particularly seen in this case (**Figure 6**).

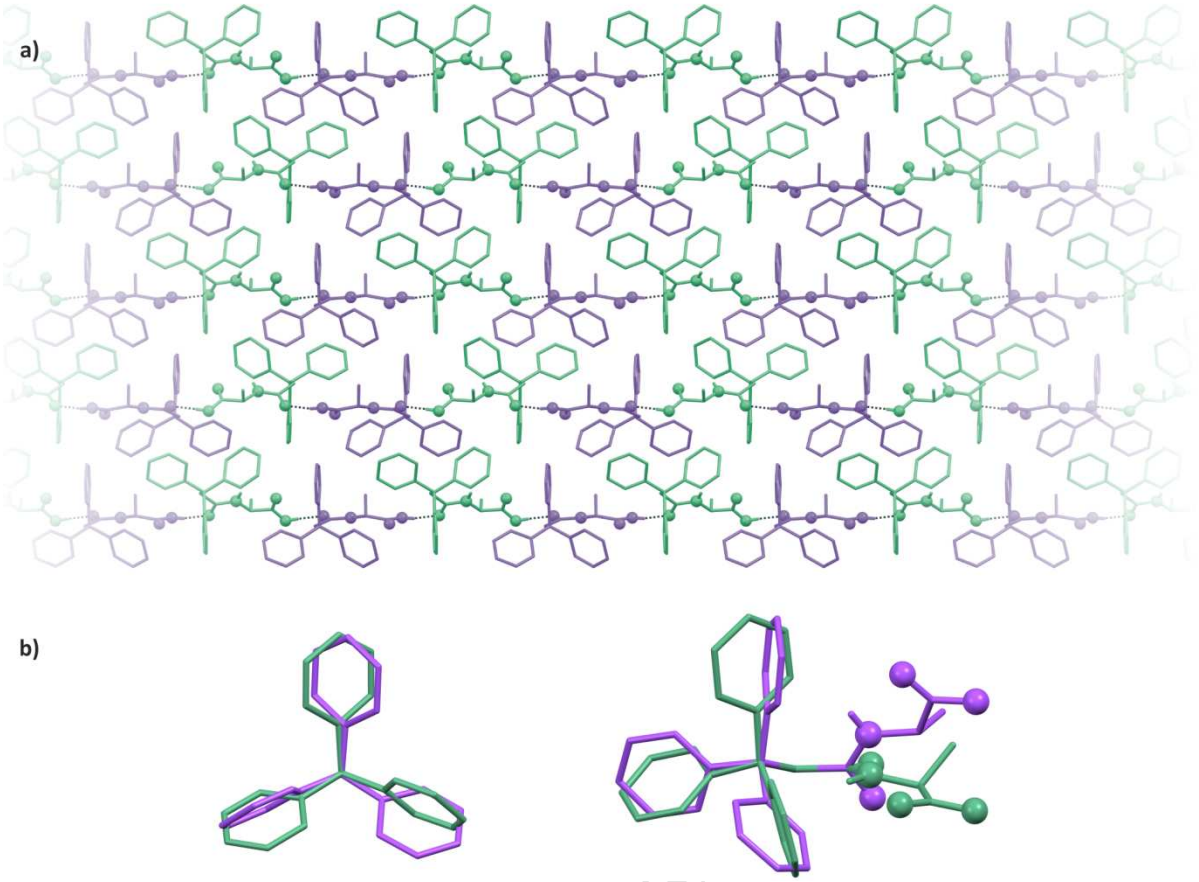


**Figure 6.** a) Molecular packing in the crystal structure of **4a** (view along x axis). b) The comparison between the conformation of symmetrically independent molecules A and B. The O and N atoms are shown as balls, hydrogen bonds are shown as a dashed line and C-bound hydrogen atoms have been omitted for clarity. Symmetrically independent molecules are shown with the use of different colors.

## 3. Conclusions

In this work, we have intended to show a complementary approach to the problem of chiral 3,3,3-triphenylpropionic acid derivatives. We have shown a possibility of chirality transfer from permanent chirality element to the stereodynamic probes in compounds, where the inductor and effector parts are separated by four bonds. Due to the cascade of weak but complementary interactions, the trityl group adopts helical conformation, which is related to the appearance of non-zero Cotton effects in the region of trityl absorption. The sign of Cotton effect appeared at about 205 nm was found dependent on absolute configuration of stereogenic center on the carbon atom in α position to the linker atom. The calculated low-energy conformers of **1a**, **1c**, **2a**, **2c**, **3a** and **3c** are characterized by *PPP* or *MMM* helicities. Therefore, we can generally determine that in the case of 3,3,3-triphenylpropionic acid derivatives, the chiral substituents generate homohelicity of the trityl group.

Taking into considerations the larger distance between inductor and reporter group, we may conclude that sensitivity to chiral environment is high. In general, the estimated dissymmetry factors $\Delta\varepsilon/\varepsilon$, which can be a measure of the sensitivity in chirogenesis, are not much smaller than those

estimated for other optically active derivatives containing trityl group (see ESI, Table S_8). For example, estimated dissymmetry factors for **2a** and for *N*-triphenylacetyl-2-amino butane are almost the same ($0.61\times10^{-4}$ and $0.62\times10^{-4}$, respectively). On the other hand, the dissymmetry factor estimated for *O*-tritylmenthol is the highest within all trityl derivatives, which have been taken into consideration so far, and equals to $11.21\times10^{-4}$, whereas estimated for triphenylsilyl ether of menthol and for **1c** equal to $1.35\times10^{-4}$ and $0.76\times10^{-4}$, respectively. While for *O*-trityl alcohols and for *N*-trityl amines the sterical interactions are the major factors responsible for chirality transfer, for *N*-triphenylacetamides the sterical interactions are supported by electrostatic interactions. In the case of chiral 3,3,3-triphenylpropionic acid derivatives the large distance between inductor and reporter is balanced by *the ordering effect* of the carbonyl group from triphenylpropionic acid moiety. This in turn reveals in the lower conformational freedom of the 3,3,3-triphenylpropionic acid derivatives in comparison to other trityl-containing and optically active compounds.

The incorporation of the trityl group allowed, to some extent, for the control over the supramolecular assembly of amide derivatives of 3,3,3-triphenylpropionic acid. Observed in the asymmetric part of the unit cell multiplication of the molecules, characterized by different conformation of trityl group, is often accomplished with pseudo-centrosymmetric type of packing. This is apparently due to the maximization of packing in the crystal lattice, where the conformational liability of trityl allows for its easy adaptation to the environment, with a small increase in the energy of an individual molecule. We expected that energetic effects associated with formation of intermolecular O-H···O hydrogen bonding would prevail over the effects associated with the strains resulting from steric congestion. Hence, the studied chiral 3,3,3-triphenylpropionic acid amides are characterized by very low ability to form microporous crystals.

On the other hand, the presence in the same molecule of two supramolecular synthons significantly different in sterical requirements and hydrophobicity led to helical superstructures previously never observed for *N*-acylamino acid derivatives or for trityl-containing compounds. In our opinion, such results constitute a convenient starting point for rational design of molecules capable of forming functional superstructures under controlled manner. Further studies are in progress in our laboratory.

## 4. Experimental section

### *4.1. General Information.*

Unless otherwise noted, all reactions were carried out in air atmosphere. Tetrahydrofuran (THF) was dried by distillation over potassium; dichloromethane was dried by distillation over calcium hydride.

Deuterated chloroform ($CDCl_3$), solvents and other chemicals, were purchased from commercial suppliers and used as received without further purification.

$^1H$ and $^{13}C\{H\}$ NMR spectra were recorded on Bruker Ascend 600 MHz or Bruker Ultrashield 300 MHz spectrometer at room temperature. Chemical shifts are reported in parts per million (ppm). Spectra are referenced using an internal reference (TMS or $CDCl_3$ residual solvent peak). Data are described as follows: chemical shift, multiplicity (s = singlet, d = doublet, t = triplet, q = quartet, m = multiplet, br = broad) and integration. Thin-layer chromatography (TLC) was carried out using Sigma-Aldrich precoated TLC plates (60 Å medium pore diameter with fluorescent indicator 254 nm). Melting points were measured on the BUCHI B-545. High resolution mass spectra (HRMS) were measured on the Bruker Impact HD. Optical rotations were recorded on the Jasco P-2000 polarimeter at 20 °C. ECD and UV spectra were measured using the Jasco J-810 spectropolarimeter at room temperature in cyclohexane and acetonitrile solution and with the use of quartz cell of the optical lengths varied from 0.05 cm to 0.1 cm. The concentration of the solutions ranged from 1.2 to $2.5\times10^{-4}$ mol $L^{-1}$. Background spectra of the pure solvents were recorded from 400 to 185 nm with a scan speed 100 nm $min^{-1}$.

For the calculation details, see Electronic Supplementary Information.

***4.2. X-ray diffraction experiment details***.

A monocrystals suitable for X-ray structural analysis were obtained by slow evaporation of chloroform (crystals of compounds **2a**-**2c**), hexane : ethyl acetate 1:1 mixture (for compounds **3a**-**3c**) or diethyl ether : chloroform 1:1 mixture (for compound **4a**). The diffraction data were collected at 130 K with an Oxford Diffraction SuperNova diffractometer using Co Kα radiation (λ = 1.54184 Å). The intensity data were collected and processed using CrysAlis PRO software. The structures were solved by direct methods and refined by full-matrix least-squares method on $F^2$. The carbon-bound hydrogen atoms were refined as riding on their carriers and their displacement parameters were set equal to 1.5Ueq(C) for the methyl groups and 1.2Ueq(C) for the remaining H atoms. The hydrogen atoms of OH and NH groups were located in electron-density difference maps. In the final cycles of refinement they were included in calculated position and treated as riding atoms, their displacement parameters were set equal to 1.5Ueq(N/O).

***4.3. Representative synthetic procedures and spectral data for 1-4***

**3,3,3-Triphenylpropionic acid** was synthesized from malonic acid and triphenylmethanol according to the procedure of Hellerman.[38] Amino acid esters hydrochlorides were prepared according to well-known general methods.[39]

**3,3,3-Triphenylpropionic acid chloride:**[43] 3g (10 mmol) of 3,3,3-triphenylpropionic acid was dissolved in 25 mL of chloroform containing a drop of DMF. To this solution, a 2.38g (20 mmol) of thionyl chloride was added drop wise. The solution was stirred overnight under reflux. After evaporation of all volatiles, 10 mL of toluene was added and the slurry was evaporated again. The crude product was obtained as a slightly yellowish solid, which was used for next reaction without purification.

**General methods for preparation of esters 1a-1e.** Representative procedure for ester **1a**: 0.5 mmol of 3,3,3-triphenylpropionic acid chloride was dissolved in 5 mL of dry dichloromethane. To this solution 50 mg (0.069 mL, 0.5 mmol) of $Et_3N$ was added, followed by 37 mg (46 µL, 0.5 mmol) of *R*-(-)-2-butanol in 5 mL of $CH_2Cl_2$. The mixture was stirred for 3h and the solvent was evaporated. Crude product was redissolved in dichoromethane, washed with 2M HCl, 5% $NaHCO_3$, water, brine and dried over $Na_2SO_4$. After evaporation to dryness, the residue colorless oil was purified by column chromatography on silica gel and using $CH_2Cl_2$ as eluent to give 116 mg (65%) of pure **1a** as an oil. $[\alpha]_D$ = -3.1 (c = 1, $CHCl_3$); ESI-MS 381.1832 $[M+Na]^+$, calc. for $C_{25}H_{26}NaO_2$ 381.1830; $^1$H NMR (600 MHz, $CDCl_3$) δ 7.30–7.20 (m, 15H), 4.61 (d, *J* = 6.2 Hz, 1H), 3.76 (d, 2H), 1.45–1.23 (m, 2H), 0.93 (d, 3H), 0.75 (t, 3H); $^{13}$C NMR (151 MHz, $CDCl_3$) δ 170.64, 146.73, 129.30, 127.76, 126.17, 72.26, 55.70, 46.80, 28.45, 18.88, 9.54; IR (ATR) $cm^{-1}$: 3052, 3032, 2934, 2871, 1728, 1595, 1494, 1444, 1347, 1200, 1152, 756, 697.

**General methods for preparation of amides 2a-2g.** Representative procedure for amide **2a**: 1 mmol of 3,3,3-triphenylpropionic acid chloride was dissolved in 10 mL of dichloromethane. To this solution 101 mg (0.139 mL, 1 mmol) of $Et_3N$ was added followed by 73 mg (100 µL, 1 mmol) of *S*-(-)-2-aminobutane in 5 mL of dichloromethane. The mixture was stirred for 3 h and then the solvent was evaporated. The crude product was redissolved in dichoromethane, washed with 2M HCl, 5% $NaHCO_3$, water, brine and dried over $Na_2SO_4$. After evaporation, the residue was purified by column chromatography on silica gel using 5% MeOH in $CH_2Cl_2$ as eluent to give 142 mg (40%) of **2a** as white crystals. M.p. = 173-174°C; $[\alpha]_D$ = +6.95 (c = 1, $CHCl_3$); ESI-MS 358.2163 $[M+H]^+$, calc. for $C_{25}H_{28}NO$ 358.2171; $^1$H NMR (300 MHz, $CDCl_3$) δ 7.48–6.98 (m, 15H), 4.57 (d, 1H), 3.7–3.5 (m, 3H C$H_2$ and C*H*), 1.08–1.00 (m, 2H), 0.70 (d, 3H), 0.62 (t, 3H); $^{13}$C NMR (75 MHz, $CDCl_3$) δ 169.76, 146.37, 129.33, 128.12, 126.50, 56.10, 49.12, 46.25, 29.07, 19.61, 10.07; IR (ATR) $cm^{-1}$: 3252, 3085, 3057, 2966, 2925, 2850, 1636, 1561, 1492, 1446, 1372, 753, 695.

**General methods of preparation of 3,3,3-triphenylpropionic acid derivatives of aminoacids esters 3a-3d.**[44] Representative procedure for **3a.** To a solution of 0.14 g (1 mmol) of L-alanine methyl ester hydrochloride and 1.5 mL of $Et_3N$ in 15 mL of $CH_2Cl_2$ was added a solution of 0.35g (1.1 mmol)

of 3,3,3,-triphenylpropionic chloride in 2 mL of $CH_2Cl_2$ with stirring at room temperature. The solution was stirred for 20 h and than evaporated to dryness. The crude solid was dissolved in 15 mL of $CH_2Cl_2$ and washed with 15 mL of saturated ammonium chloride solution, 10 mL of water, 10 mL of brine, dried over $Na_2SO_4$ and filtered. The crude product was purified by column chromatography on silica gel using 1% MeOH in $CH_2Cl_2$ or hexane:ethyl acetate (2:1) for others. The pure product was dissolved in hexane with a small amount of $CH_2Cl_2$. Crystallization provided 0.02 g of pure crystals of **4a** (5%). Mp = 170-172 °C; ESI-MS 388.1929 $[M+H]^+$ calc. for $C_{25}H_{26}NO_3$ 388.1913; $^1$H NMR (300 MHz, $CDCl_3$) δ 0.95–0.98, (d 3H), 3.47 (d, 2H), 3.63 (s, 3H), 3.72 (d, 1H), 4.27 (m, 1H), 5.35 (d, 1H), 7.29 (m, 15H), $^{13}$C NMR (101 MHz, $CDCl_3$) δ 17.80, 47.84, 48.57, 52.23, 56.5, 126.46, 128,08, 129.25, 146.26, 169.88, 173.02; IR (ATR) $cm^{-1}$: 3265, 3084, 1745, 1640, 1557, 1213, 1158, 744, 612.

**General methods of preparation for 3,3,3-triphenylpropionic acid derivatives of amino acids 4a-4e.** Representative procedure for **4a**: 445 mg (5 mmol) of L-alanine was dissolved in 20 mL of water containing NaOH (0.4 g, 10 mmol) and THF (5 mL). Then 3,3,3-triphenylpropionic acid chloride (1.05 g, 3.27 mmol) was added and the whole mixture was stirred for 2 h. The solution was gently acidified with hydrochloric acid and the forming precipitate and the remaining solution was extracted several times with ethyl acetate. Organic phase was separated and dried over $Na_2SO_4$. After removal of solvent, the crude product was purified by column chromatography on silica gel and with the use of hexane:ethyl acetate (2:1) as eluent, yielding 268 mg (22%) of the pure **4a** as white solid. M.p. = 187-188 °C; $[\alpha]_D$ -120.5 (c = 1, $CHCl_3$); ESI-MS 374.1763 $[M+H]^+$, calc. for $C_{24}H_{24}NO_3$ 374.1756; $^1$H NMR (300 MHz, DMSO-$d_6$) δ 0.94 (d. 3H), 3.43–3.48 (d. 2H), 3.77-3.90 (m. 1H), 7.21 (m. 15H), 7.84 (d. 1H), 12.36 (s. 1H); $^{13}$C NMR (75 MHz, DMSO-$d_6$) δ 17.49, 46.48, 4.56, 56.26, 126.19, 127.87, 129.67, 147.65, 169.77, 174.44; IR (ATR) $cm^{-1}$: 3303, 3057, 2962, 1745, 1643, 1537, 1203, 1147.

## Declarations of interest

The authors declare no competing financial interest.

## Acknowledgments

This work was supported by a research grant from National Science Center (NCN) Poland, Grant UMO-2016/21/B/ST5/00100. All calculations were performed in Poznan Supercomputing and Networking Center (grant no 406).

## Appendix A. Supplementary data

Calculations details; Tables S_1-S_7, Figures S_1-S_50; copies of $^1$H and $^{13}$C NMR spectra; copies of ECD spectra; Cartesian coordinates for all calculated low-energy structures.

CCDC 1908897-1908903 contains the supplementary crystallographic data for this paper. These data can be obtained free of charge via www.ccdc.cam.ac.uk/data_request/cif, or by email data_request@ccdc.cam.ac.uk, or by contacting The Cambridge Crystallographic Data Centre, 12 Union Road, Cambridge CB2 1EZ, UK; fax: +44 1223 336033.

**References**

[1] *Comprehensive Asymmetric Catalysis*. Jacobsen, E. N.; Pfaltz, A.; Yamamoto, H. Eds.; Springer: Berlin, Heidelberg, 2004.

[2] *Chirality in Natural and Applied Science*. Lough, W. J.; Wainer, I. W. Eds.; CRC Press: Boca Raton, 2002.

[3] *Comprehensive Chiroptical Spectroscopy (Applications in Stereochemical Analysis of Synthetic Compounds, Natural Products, and Biomolecules)*. Berova, N.; Polavarapu, P. L.; Nakanishi K.; Woody, R. W. Eds.; Wiley: Hoboken, 2012.

[4] Flack, H. D; Bernardinelli, G. *Chirality* 2008, 20, 681 and references cited therein.

[5] Feringa, B. L. *Angew. Chem. Int. Ed.* 2017, 56, 11060 and references cited therein.

[6] Sauvage, J-P. *Angew. Chem. Int. Ed.* 2017, 56, 11080 and references cited therein.

[7] Stoddart, J. F. *Angew. Chem. Int. Ed.* 2017, 56, 11094 and references cited therein.

[8] Mislow, K. *Acc. Chem. Res.* 1976, 9, 26.

[9] Iwamura, H.; Mislow, K. *Acc. Chem. Res*. 1988, 21, 175.

[10] Berg, U.; Liljefors, T.; Roussel, C.; Sandström, J. *Acc. Chem. Res*. 1985, 18, 80.

[11] Rappoport, Z.; Biali, S. E. *Acc. Chem. Res.* 1997, 30, 307.

[12] Greene, T. W.; Wats, P. G. M. *Protective Groups in Organic Synthesis*. Wiley: New York, 2006, pp. 152-156.

[13] Bah, J.; Franzén J. *Chem. Eur. J*. 2014, 20, 1066.

[14] Ni, S.; El Remaily, M. A. E. A. A. A.; Franzén, J. *Adv. Synth. Catal.* 2018, 360, 4197.

[15] Khazaeia, A.; Zolfigol, M. A.; Moosavi-Zare, A.R.; Zare, A.; Parhami, A.; Khalafi-Nezhad, A. *Applied Catal. A: General*, 2010, 386, 179.

[16] Khazaei, A.; Zolfigol, M. A.; Moosavi-Zare, A. R.; Abi, F.; Zare, A.; Kaveh, H.; Khakyzadeh, V.; Kazem-Rostami, M.; Parhami, A.; Torabi-Monfared, H. *Tetrahedron*, 2013, 69, 212.

[17] Khazaei, A.; Zolfigol M. A.; Moosavi-Zare, A. R.; Zare, A.; Khojasteh, M.; Asgari, Z.; Khakyzadeh, V.; Khalafi-Nezhad, A. *Catal. Commun*. 2012, 20, 54.

[18] Ishikawa, K.; Tohyama, K.; Mitsuhashi, S.; Maruta, S. *J. Biochem.* 2014, 155, 257.

[19] Kaan, H. Y.; Weiss, J.; Menger, D.; Ulaganathan, V.; Tkocz, K.; Laggner, C.; Popowycz, F.; Joseph, B.; Kozielski, F. *J. Med. Chem*. 2011, 54, 1576.

[20] Wu, W.; Jingbo, S.; Xu, W.; Liu, J.; Huang, Y.; Sheng, Q.; Lv, Z. *Oncology Lett*. 2018, 16, 1023.

[21] Zhai, W.; Feng, Y.; Liu, H.; Rockenbauer, A.; Mance, D.; Li, S.; Song, Y.; Baldus, M.; Liu, Y.; *Chem. Sci.* 2018, 9, 4381.

[22] Carotti, A.; Ianni, F.; Camaioni, E.; Pucciarini, L.; Marinozzi, M.; Sardella, R.; Natalini, B. *J. Pharm. Biomed. Anal.* 2017, 144, 31.

[23] Wolf, C. *Dynamic Stereochemistry of Chiral Compounds: Principles and Applications*, Royal Society of Chemistry: Cambridge, 2008.

[24] Schuster, J. J.; Colter, A. K.; Kurland, R. J. *J. Am. Chem. Soc.* 1968, 90, 4676.

[25] Jones, P. G.; Sheldrick, G. M.; Edwards, M. R.; Kirby A. J. *Acta. Cryst.* 1986, C42, 1361.

[26] Kurland, R. J.; Schuster, J. J.; Colter, A. K.; *J. Am. Chem. Soc.* 1965, 87, 2279.

[27] Ściebura, J.; Skowronek, P.; Gawroński, J.; *Angew. Chem. Int. Ed*. 2009, 48, 7069.

[28] Ściebura, J.; Gawroński, J.; *Chem. Eur. J*. 2011, 17, 13138.

[29] Ściebura, J.; Janiak, A.; Stasiowska, A.; Grajewski, J.; Gawrońska, K.; Rychlewska, U.; Gawroński, J. *ChemPhysChem* 2014, 15, 1653.

[30] Prusinowska, N.; Bendzińska-Berus, W.; Jelecki, M.; Rychlewska, U.; Kwit, M. *Eur. J. Org. Chem*. 2015, 4, 738 and references therein.

[31] Prusinowska, N.; Bendzińska-Berus, W.; Szymkowiak, J.; Warżajtis, B.; Gajewy, J.; Jelecki, M.; Rychlewska, U.; Kwit, M. *RSC Adv*. 2015, 5, 83448.

[32] Skowronek, P.; Ścianowski, J.; Pacuła, A. J.; Gawroński, J. *RSC Adv*. 2015, 5, 69441.

[33] Wolf, C.; Bentley, K. W. *Chem. Soc. Rev*. 2013, 42, 5408.

[34] Wang, L.; Zhang, T.; Redden, B. K.; Sheppard, C. I.; Clark, R. W.; Smith, M. D.; Wiskur, S. L. *J. Org. Chem.* 2016, 81, 8187.

[35] Bendzińska-Berus, W.; Warżajtis, B.; Gajewy, J.; Kwit, M.; Rychlewska, U. *Cryst. Growth Des.* 2017, 17, 2560.

[36] Megumi, K.; Yokota, S.; Matsumoto, S.; Akazome, M. *Tetrahedron Lett.* 2013, 54, 707.

[37] Akazome, M. *Chiral Recognition by Inclusion Crystals of Amino-Acid Derivatives Having Trityl Groups*. In *Advances in Organic Crystal Chemistry*. R. Tamura, M. Miyata, Eds.; Springer: Berlin 2015; Chapter 23, pp. 463-482 and references therein.

[38] Hellerman, L. *J. Am. Chem. Soc.* 1927, 49, 1735.

[39] *Preparatyka i elementy syntezy organicznej*; Wróbel J. Ed. PWN, Warszawa, 1983.

[40] Mądry, T.; Czapik, A.; Kwit, M. *ACS Omega* 2019, 4, 3244.

[41] Rodger, A.; Nordén, B. *Circular Dichroism & Linear Dichroism*. Oxford University Press Inc.: New York, 1997.

[42] TD-CAM-B3LYP/6-311++G(d,p)//B3LYP/6-311++G(d,p) level. Gaussian 09, revision D.01; Gaussian, Inc.: Wallingford, CT, 2009.

[43] Gibson, H. W.; Liu, S.; Lecavalier, P.; Wu, C.; Shen, Y. X. *J. Am. Chem. Soc.* 1995, 117, 852.

[44] Zhao, X.; Jiang, X.-K.; Shi, M.; Yu, Y.-H.; Xia, W.; Li. Z.-T. *J. Org. Chem*. 2001, 66, 7035.